

## Photofission at CEBAF Energies

B.L. Berman, K.S. Dhuga, and W.R. Dodge

Center for Nuclear Studies, The George Washington University  
and

B.G. Ritchie

Department of Physics and Astronomy, Arizona State University

This CLAS Note outlines a proposed photofission experiment using the CLAS and its tagged-photon beam. We solicit comments, criticisms, and especially expressions of interest from the CEBAF community.

### I. Motivation

At photon energies from above the giant dipole resonance (GDR) through the delta region, there is evidence that the photofission cross section for the uranium isotopes is very nearly as large as the total photonuclear cross section. This means that if such a nucleus absorbs a photon in this energy range, it almost always fissions, sooner or later (although it can emit other particles, such as evaporation neutrons, prior to fissioning). Since the fission process liberates about 200 MeV in addition to the energy of the incident photon, a fission event is easy to detect, e.g., with parallel-plate avalanche counters (PPACs). Thus, one can measure at least a good approximation to the photonuclear absorption cross section by detecting fission events with a relatively simple and inexpensive detector which can have an efficiency of nearly 100%.

Probably this property of the uranium isotopes and other very heavy nuclei, namely that photon absorption almost always leads to fission, persists to CEBAF energies, and thus would make possible a relatively painless method for determining the total photonuclear cross section—in itself a worthy goal. One could irradiate uranium-loaded PPACs with tagged photons and get a good measure of the total cross section as a function of photon energy from below the delta to a few GeV, with important implications for the onset of hadronization, shadowing, and vector-meson dominance.

But what if on occasion photon absorption does not lead to fission? One then would have to explain how a uranium nucleus could absorb a GeV photon, emit particles (presumably from the surface), and result in a cold, non-fissile residual nucleus. [Note that as neutrons are emitted, the fissionability, which is proportional to  $Z^2/A$ , increases, although if an n-p pair is emitted, the fissionability decreases somewhat.] What kind of mesons and/or resonances would be produced under such a constraint? In order to explore the branching to and nature of such events, one needs to detect the other emitted particles, in anticoincidence with fission fragments. This is an ideal experiment for CLAS, using tagged photons and thin-walled (and low-Z) uranium-loaded (as well as empty) PPACs in the target position. The observation and delineation of such unusual events perhaps could lead to the discovery of unanticipated and interesting new phenomena.

## II. Background

At low energies, through the GDR region, the wavelength of the incident photon (about 20 fm at 10 MeV) is comparable to the size of the nucleus (about 15 fm). Here, the photofission cross sections for the eight longest-lived actinide nuclei have been measured with high accuracy using monoenergetic photons (from the annihilation in flight of fast positrons), and certain other properties of the fission process have been delineated as well (Refs. 1-5). Figures 1 and 2 show the photonuclear cross sections for  $^{235}\text{U}$  and  $^{238}\text{U}$ , respectively (Ref. 3), showing that the photofission cross section for the former is larger than that for the latter. Figure 3 shows the fission probability  $P_{F_1}$  (first-chance fission only) at low energies for four actinide nuclei (Ref. 3), showing that  $^{232}\text{Th}$  is even less fissionable than  $^{238}\text{U}$ . Figure 4 shows the ratio of neutron and fission widths for all of the low-energy photofission data (a total of ten nuclei; from Ref. 5), showing the steep dependence of this quantity on fissionability. It can be seen that even at low energies, the fission probability for some nuclei (namely  $^{233}\text{U}$  and  $^{239}\text{Pu}$ ) exceeds 70%.

Above the GDR, the total photofission cross section becomes an increasingly large fraction of the absorption cross section, owing mainly to the increasing importance of multiple-chance fission. Already at 18 MeV, second-chance fission for  $^{236}\text{U}$  and  $^{238}\text{U}$  is as probable as first-chance fission (Ref. 2).

In the quasideuteron energy region, from about 30 to 130 MeV, the photon wavelength (2 fm at 100 MeV) is comparable to the internucleon spacing in the nucleus (about 2 fm). Here, there are fewer data, with larger uncertainties; but those that exist (Refs. 6-8, but also see Ref. 9) show that the total photofission cross section, at least for  $^{235}\text{U}$  and  $^{238}\text{U}$ , is practically equal to the total photonuclear cross section (Ref. 10) in this energy region. Figure 5 shows the photofission cross section for  $^{238}\text{U}$  and  $^{235}\text{U}$ , obtained with tagged bremsstrahlung (Ref. 6), and compares the former with the total photonuclear cross section, obtained with annihilation photons, showing that within the rather large error limits (of Ref. 10) the two cross sections are about the same. Figure 6 shows the deduced total fission probabilities  $P_{F_T}$  (Ref. 7), showing that for these two nuclei they are close to unity in this energy region, and that even for  $^{232}\text{Th}$   $P_{F_T}$  becomes as large as about 0.7. Perhaps one should not be surprised at these large values, because a nucleon from the n-p pair which absorbs the photon, especially a low-energy proton, is often reabsorbed by Coulomb or other final-state interactions in such a large nucleus.

In the delta energy region, from about 140 to 500 MeV, the photon wavelength (0.66 fm at 300 MeV) is comparable to the size of the nucleon itself. Here, the data are very sparse, with only two photofission measurements with monoenergetic photons (Refs. 11 and 12), to be compared with only two comparable photoabsorption measurements (Refs. 13 and 14). Figure 7 shows the total photonuclear absorption cross section per nucleon (Ref. 14), derived from data for Be and Pb, showing that they are nearly the same. Figure 8 compares these data with the photofission data of Ref. 11, obtained with tagged photons, and Fig. 9 adds in the photofission data of Ref. 12, obtained with annihilation photons. Both of these figures show that the photofission cross sections per nucleon for  $^{235}\text{U}$  and  $^{238}\text{U}$  are about the same as each other (but not quite), and that they are almost as large (but not quite) as the photoabsorption cross sections per nucleon in this energy region. It

should be noted (in Fig. 8) that the size and shape of the *photonucleon* cross section (from Ref. 15) is much different from the *photonuclear* cross section divided by A.

Above the delta resonance, up to about 800 MeV, there are some new data on  $^{238}\text{U}$  obtained with tagged photons at Mainz. The first preliminary results of this measurement are shown in Fig. 10 (Ref. 16). One sees a certain lumpiness in the data between 500 and 700 MeV, which presumably reflects the excitation of other nucleon resonances in this energy region.

At CEBAF energies, up to about 4 GeV, the photon wavelength can be as small as 0.05 fm, smaller than the presumed size of a constituent quark. Here, only a single photofission experiment has been performed (Refs. 17), with tagged photons but poor statistics. These data are shown in Fig. 11, together with the lowest two (out of six) data points for the total hadron photoproduction of Ref. 18. Within the (large) experimental uncertainties, they look the same. By comparing their *average* data with the total *photonucleon* hadronic cross section (Ref. 19), the authors of Ref. 16 infer a screening parameter which they claim to be accurate to 0.5%. Clearly, more and especially better data, both photofission and photoabsorption, are called for in this energy region. We propose here to obtain such data at the CLAS.

### III. Proposed Experiment

Somewhere around 600 MeV, the pair of nucleons from quasideuteron absorption achieve their longest mean-free path in nuclear matter, and hence would be most likely to escape the nucleus without rescattering, thus lowering  $P_{FT}$ ; but the photon wavelength here (0.33 fm) is not well matched to the internucleon spacing. Somewhere around 1.5-2.0 GeV (0.13-0.10 fm), the photoproduction of nucleon resonances no longer dominates the photoabsorption process. Somewhere around 4-5 GeV (0.05-0.04 fm), the incident photon becomes hadron-like in its behavior, signalling the onset of nuclear shadowing (Ref. 18). Clearly, throughout the CEBAF energy range, the study of photofission and photonuclear absorption will very likely lead to interesting results.

The questions to be answered, as a function of photon energy, for heavy nuclei, are:

1) Is  $P_{FT}$  nearly equal to unity? If so, photofission is a good measure of total photonuclear absorption.

2) If so, what are the implications for shadowing, and for various sum rules?

3) If not, what is the branching ratio for non-fission events, and what is their nature? What kinds of processes leave the residual nucleus cold? Do such processes take place preferentially on the nuclear surface? What is the effect of the nuclear medium on such processes? Are strong many-body forces important?

The experiment would consist of the irradiation of PPACs placed in the standard target location in the CLAS with tagged photons. We would use as a minimum one uranium isotope and an unloaded PPAC. The particles (primarily charged particles) detected by the CLAS in coincidence with fission fragments detected by the PPAC would characterize a fission event and enable us to subtract background events more effectively than by using

the unloaded-PPAC alone for our background determination. The particles detected by the CLAS in anticoincidence with a fission fragment would characterize those presumably very interesting events that result in a cold residual nucleus. It is desirable to have the primary electron beam as high in energy as possible, in order to tag the largest possible range of incident photon energies, although the experiment can be run and would be valuable at any reasonable electron beam energy. Since it would be desirable to overlap the existing data in the delta region, some data should be obtained as well with a relatively low electron beam energy, of 1.25-1.5 GeV.

It should be noted that the photofission cross section itself, as well as many of the other experimental details, such as beam monitoring and the like, can be measured in advance of the installation of the CLAS itself, and in this way constitute a very valuable first test of much of the ancillary equipment needed for CLAS experiments. The crucial non-fission events, however, cannot be measured without the CLAS.

#### IV. Relation to Other CEBAF Experiments

The physics interests outlined above significantly overlap those of proposal 89-002 (Ref. 20). That proposal envisions measurements of the energy and A-dependence of total hadronic cross section for photons. The method proposed there requires detection of all charged outgoing hadrons (with the CLAS) resulting from the incidence of 0.5- to 3.0-GeV photons on hydrogen, deuterium, beryllium, carbon, oxygen, aluminum, copper, tin, and lead targets. The physics issues of shadowing, isobar production, and vector dominance that are pertinent to those measurements are also relevant to the understanding of the mechanisms responsible for the dominant role played by fission in the total hadronic cross sections. The photon energy region to be explored in 89-002 also will overlap that for this proposal.

Several phenomena of interest to experiments proposed by the Nucleon-Resonance and Multi-Hadron Collaborations may also appear in the data to be taken here. One example would be how the underlying nucleon resonances manifest themselves in the total hadronic and photofission cross sections. For instance, the modification of the delta resonance in nuclear matter and the degrees of freedom appropriate to a description of any such modification are targeted for study in proposals 89-017 (Ref. 21) and 89-037 (Ref. 22). Yet these phenomena also could be explored by their influence on the total photofission and hadronic cross sections in the measurements outlined here. The extension of these ideas from the delta resonance to other nucleon resonances could be made from the measurements to be obtained in proposals 89-032 (Ref. 23) and 89-036 (Ref. 24), which will study the local and short-range properties of nuclear matter via backward particle production, and proposals 89-039 (Ref. 25) and 91-008 (Ref. 26), which should provide insight into the isospin-1/2 content of the nucleon-resonance spectrum via eta and eta' electro- and photoproduction.

As outlined in this brief discussion, the photofission measurements sketched above will complement and supplement the knowledge base obtained from a broad spectrum of CEBAF experiments, and will thus be extremely useful in exploring and extending many

of the fundamental questions to be answered with CEBAF concerning the structure of the nucleon and the modification of its behavior in the nuclear medium.

### V. Relation to Experiments Elsewhere

The experimental work proposed here is closely related to the similar measurements proposed for the jet-target tagged-photon facility at Frascati (Ref. 27). In fact, both the goal of determining the total photon absorption cross section and that of determining the relative fissilities of various heavy nuclei are included in the Frascati program; the obvious distinguishing feature is the fact that the Frascati photon beam energy is limited to 1.2 GeV (their energy resolution is also limited, to about 1%, but it is not clear that this is an important limitation for these measurements).

Some experimental work on photofission in the GeV region has been undertaken as well at Novosibirsk (Ref. 28), but it is not clear at this time that the absolute cross-section scale is under control, partly because the emphasis has been on relative fissilities (of  $^{237}\text{Np}$  and  $^{238}\text{U}$ ) and on the probability of emission of a light particle coincident with a photofission event (Refs. 29).

### VI. Note on the Fission-Fragment Detectors

Parallel-plate avalanche counters (PPACs) were used to detect the fission fragments in the NIST-Bates-Lund (NBL) electrofission experiment carried out recently at the Bates Accelerator (Ref. 30). Except for problems associated with a pulsed, high-current electron beam, these detectors performed extremely well, and certainly are the detectors of choice, not only for the experiment proposed here, but for any electrofission experiment to be proposed subsequently. Figure 12 shows the dimensions of the individual PPACs, which were arranged to cover the entire backward hemisphere. The entrance window was 0.635-mm aluminized Mylar. An equal mixture of argon and isobutane was used as the filling gas.

The spatial resolution of the fission fragments was defined by the PPAC area in the NBL experiment. However, the significant technological advances which have occurred subsequently in the use of resistive films and sheets in the construction of straw chambers should make it possible to improve greatly the spatial resolution of the PPACs that we develop for this experiment. Briefly, the policy decision by the SSC to make straw chambers a preferred technology has focused attention and funding on these devices. The use of iodine-doped Kapton as the straw-chamber wall material offers the potential to resistively divide the charge between the ends of the straw chamber, thus obtaining very good position information along the *axis* of the device. Previous problems with the erosion of plated metallic aluminum caused by the heavily ionizing fission fragments are no longer a problem with the conductive Kapton. Fast pulse information is preserved by plating a metallic coating on the *outside* of the Kapton in a geometry which also preserves the axial position information. This technology can be extended to the construction of position-sensitive PPACs in an obvious way.

## VII. Note on Counting Rates

The expected counting rates for photofission are large because the expected cross sections are large for very large nuclei. Using a cross section of 30 mb (see Fig. 11), a sample-foil thickness of 0.2 mg/cm<sup>2</sup>, a tagged-photon flux of  $3 \times 10^7 \text{ sec}^{-1}$ , and a fission-fragment detector efficiency of 100%, one obtains a counting rate of 0.5 sec<sup>-1</sup>. At this rate, 100 energy bins each with 3% statistics will require about 60 hours of data-taking, to which must be added appropriate background (sample-blank) and calibration runs. Since the sample foil can be tilted at a small angle with respect to the incident photon beam, thus making it thick to photons while keeping it thin to the emerging fission fragments, a factor of ten in effective thickness can be readily achieved, resulting in even smaller beam-time requirements.

### References

1. A. Veyssi re et al., Nucl. Phys. A199, 45 (1973)
2. J.T. Caldwell et al., Nucl. Sci. Eng. 73, 153 (1980)
3. J.T. Caldwell et al., Phys. Rev. C 21, 1215 (1980)
4. H. Ries et al., Phys. Rev. C 29, 2346 (1984)
5. B.L. Berman et al., Phys. Rev. C 34, 2201 (1986)
6. H. Ries et al., Phys. Lett. 139B, 254 (1984)
7. A. Lepr tre et al., Nucl. Phys. A472, 533 (1987)
8. R. Bernabei et al., Nuovo Cim. 100A, 131 (1988)
9. J.B. Martins et al., Phys. Rev. C 44, 354 (1991)
10. A. Lepr tre et al., Nucl. Phys. A367, 237 (1981)
11. J. Ahrens et al., Phys. Lett. 146B, 303 (1984)
12. V. Bellini et al., Nuovo Cim. 85A, 75 (1985)
13. J. Arends et al., Phys. Lett. 98B, 423 (1981)
14. C. Chollet et al., Phys. Lett. 127B, 331 (1983)
15. D. Menze et al., Physics Data 7-1 (1977)
16. U. Kneissl et al., Ann. Rep. Strahlenzentrum Univ. Giessen, p. 27 (1991)
17. E.A. Arakelyan et al., Sov. J. Nucl. Phys. 52, 878 (1990); also see E.A. Arakelyan et al., Sov. J. Nucl. Phys. 49, 780 (1989)
18. S. Michaelowski et al., Phys. Rev. Lett. 39, 737 (1977)
19. T.A. Armstrong et al., Nucl. Phys. B41, 445 (1972)
20. D.I. Sober et al., "Shadowing of Real Photons in Nuclei: Measurement of the Total Hadronic Cross Section" (1989, deferred)
21. R.M. Sealock et al. "Electroexcitation of the Delta(1232) in Nuclei" (1989, conditionally approved)
22. V. Burkert et al., "Electroproduction of the P33(1232) Resonance" (1989, conditionally approved)

23. V.B. Gavrilov et al., "Study of Local Properties of Nuclear Matter in Electron-Nucleus and Photon-Nucleus Interactions with Backward Particle Production Using the CLAS Detector" (1989, conditionally approved)
24. K.S. Egiyan et al., "Study of Short-Range Properties of Nuclear Matter in Electron-Nucleus and Photon-Nucleus Interactions with Backward Particle Production Using the CLAS Detector" (1989, conditionally approved)
25. S. Dytman et al., "Amplitudes for the S11(1535) and P11(1710) Resonances from an  $ep \rightarrow e'p \eta$  Experiment" (1989, approved)
26. B.G. Ritchie et al., "Photoproduction of  $\eta$  and  $\eta'$  Mesons" (1991, approved)
27. M. Anghinolfi et al., Frascati preprint LNF-91/089 (IR) (1991)
28. A.A. Kazakov et al., JETP Lett. 40, 445 (1984)
29. D.I. Ivanov et al., Novosibirsk preprints INP 686 and 687 (1991)
30. K. Hansen et al., Phys. Rev. C 41, 1619 (1990)

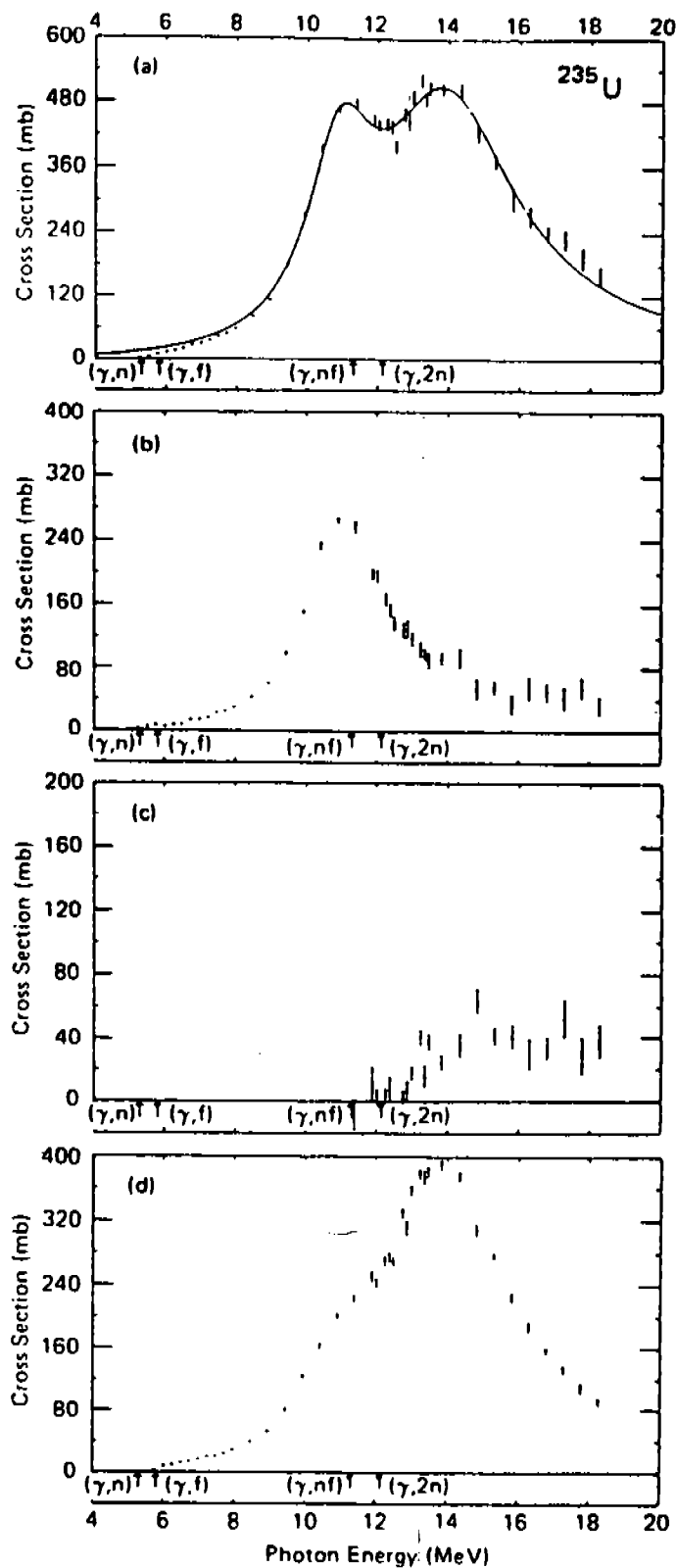


FIG. 2. Photonuclear cross sections for  $^{235}\text{U}$ : (a) total photonuclear cross section  $\sigma(\gamma, \text{tot}) = \sigma[(\gamma, n) + (\gamma, 2n) + (\gamma, F)]$ , together with a two-component Lorentz-curve fit to the data in the GDR energy region; (b) single-photon neutron cross section  $\sigma(\gamma, n)$ ; (c) double-photon neutron cross section  $\sigma(\gamma, 2n)$ ; (d) photofission cross section  $\sigma(\gamma, F)$ .

Fig. 1



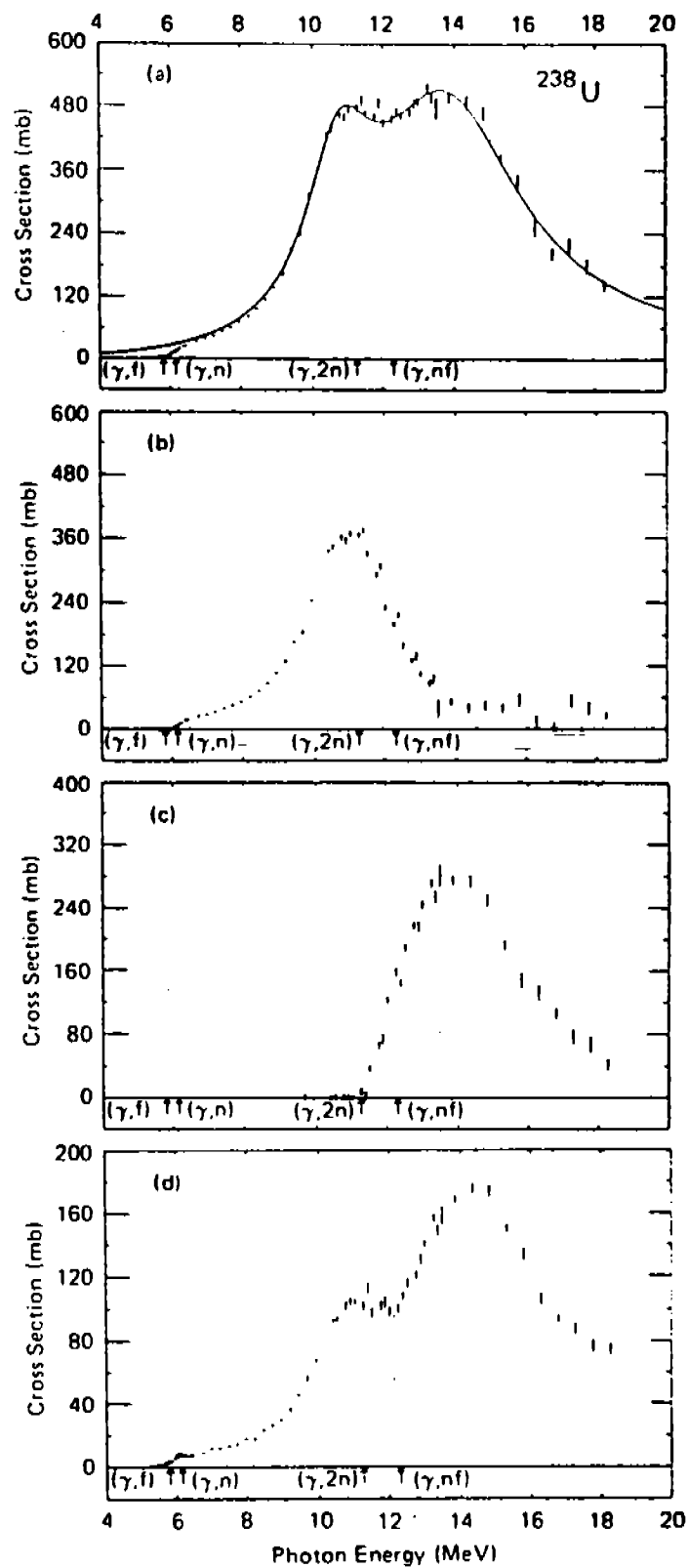


FIG. 4. Photonuclear cross sections for  $^{238}\text{U}$ : (a)  $\sigma(\gamma, \text{tot})$ , with a Lorentz-curve fit; (b)  $\sigma(\gamma, n)$ ; (c)  $\sigma(\gamma, 2n)$ ; (d)  $\sigma(\gamma, F)$ .

Fig. 2

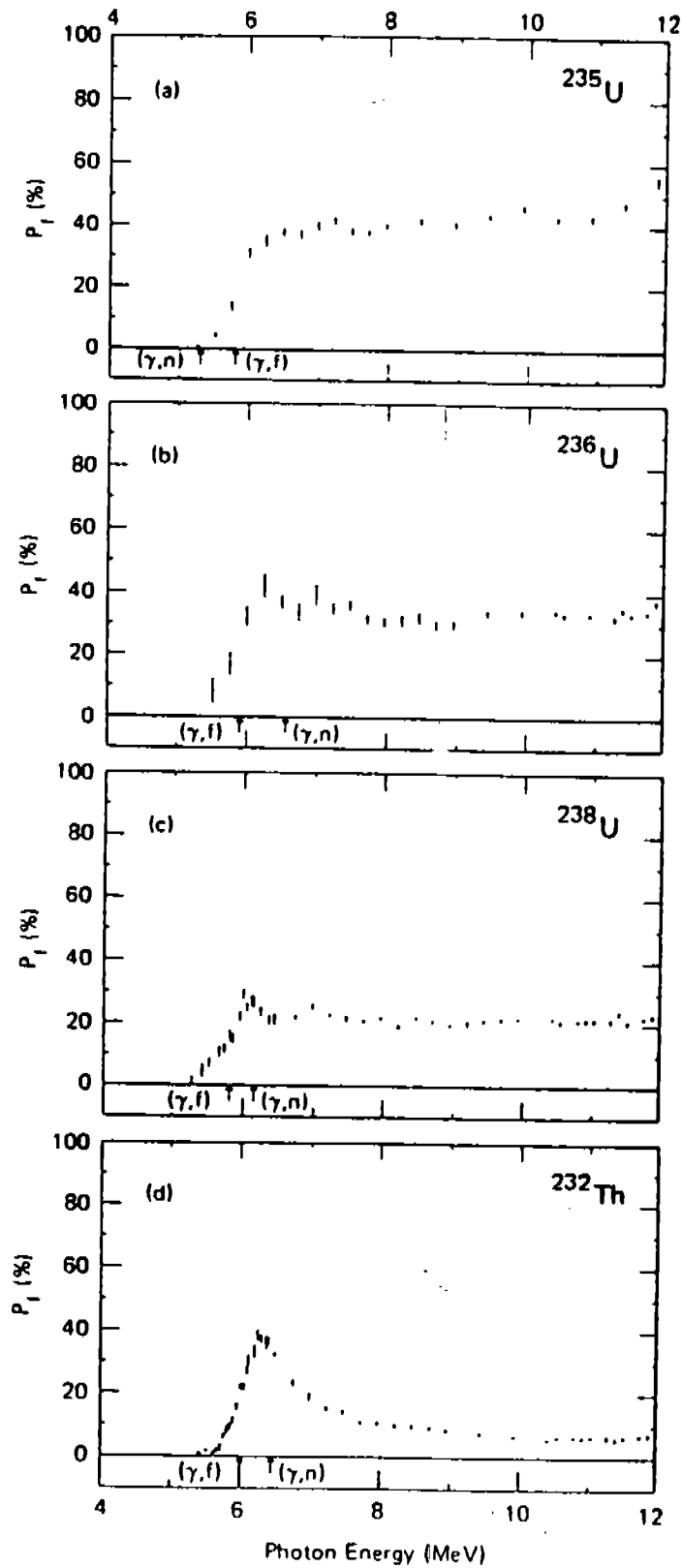


FIG. 15. Fission probability  $P_f$  from the ratio of  $\sigma(\gamma f)$  to the value at each energy of the two-component Lorentz-curve fits to the GDR shown in Figs. 2-5: (a) for  $^{235}\text{U}$ , (b) for  $^{236}\text{U}$ , (c) for  $^{238}\text{U}$ , (d) for  $^{232}\text{Th}$ .

Fig. 3

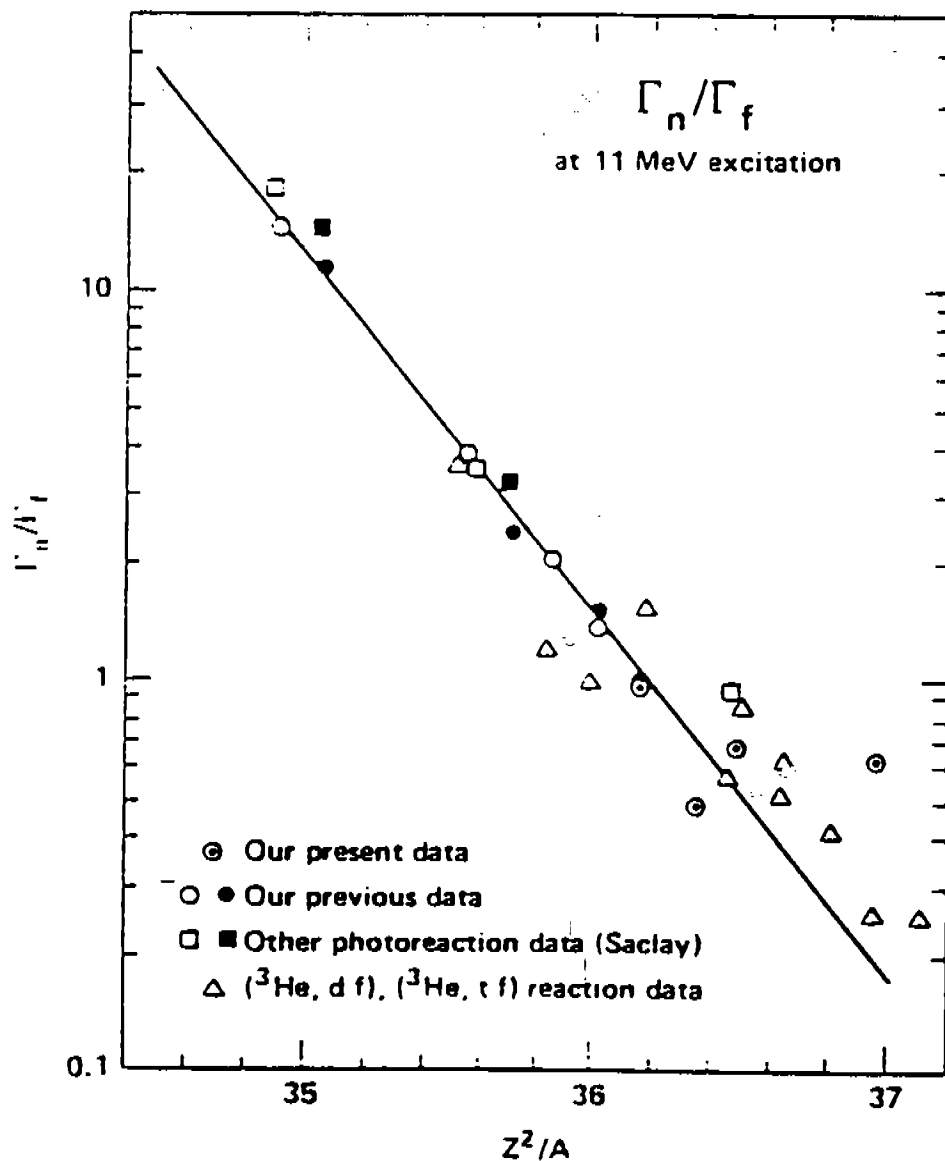


FIG. 13. Neutron-to-fission branching ratio  $\Gamma_n/\Gamma_f$  at 11-MeV excitation energy vs nuclear fissionability  $Z^2/A$ : circled dots—present work, from  $\sigma(\gamma, n)/\sigma(\gamma, f)$ ; open circles—work of Ref. 7, from  $\sigma(\gamma, n)/\sigma(\gamma, f)$ ; solid circles—work of Ref. 7, from  $\sigma(\gamma, 2n)/\sigma(\gamma, nf)$ ; open squares—work of Ref. 9, from  $\sigma(\gamma, n)/\sigma(\gamma, f)$ ; solid squares—work of Ref. 9, from  $\sigma(\gamma, 2n)/\sigma(\gamma, nf)$ ; triangles—work of Ref. 38, from ( $^3\text{He}, d f$ ) and ( $^3\text{He}, t f$ ) reactions.

Fig. 4

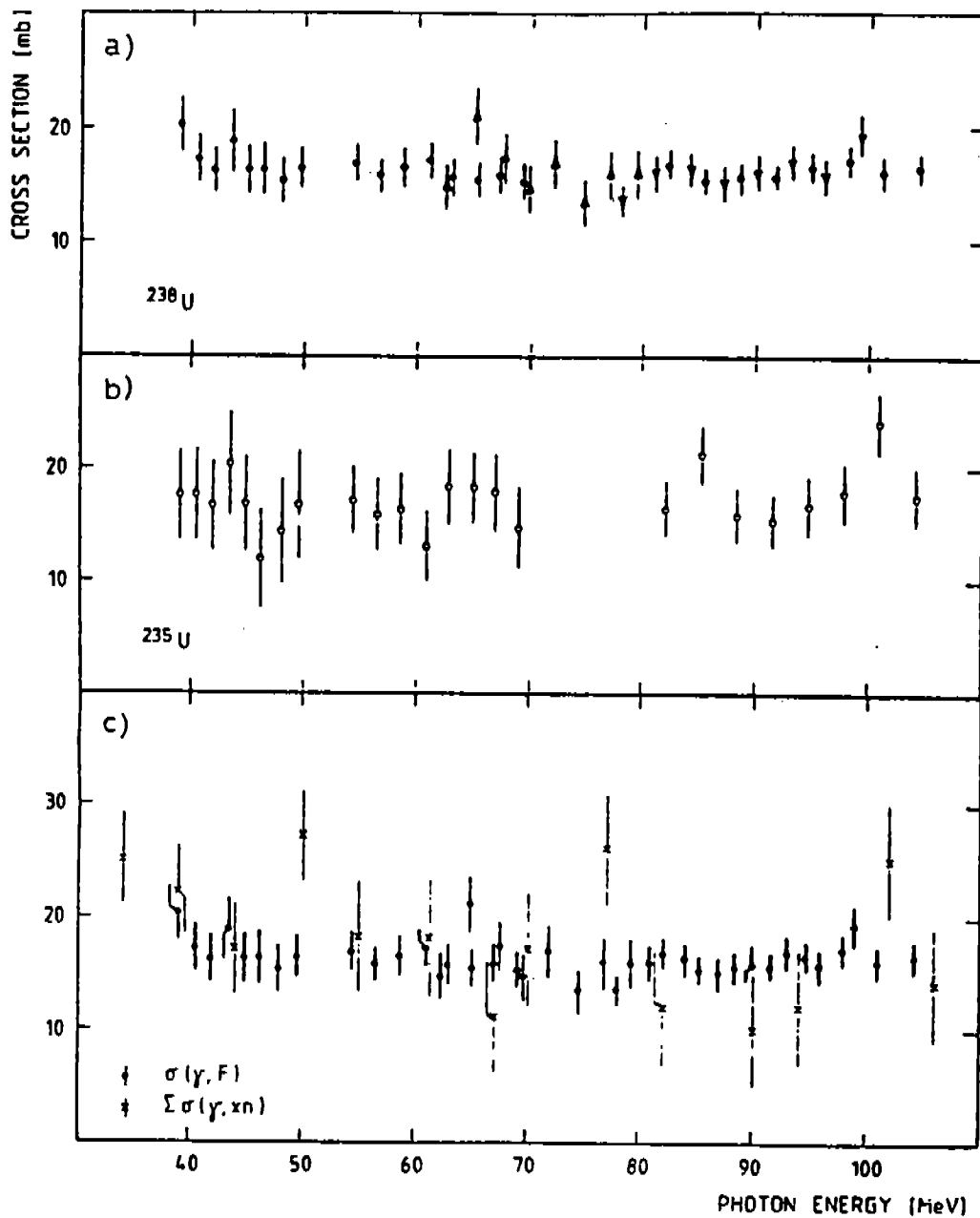


Fig. 2. (a) Photofission cross sections for  $^{238}\text{U}$  (present work). Different symbols correspond to different experimental runs. (b) Photofission cross sections for  $^{235}\text{U}$  (present work). (c) Comparison of photofission and total photon neutron cross sections [5] for  $^{238}\text{U}$ . The quoted error bars contain both statistical and systematic uncertainties.

Fig. 5

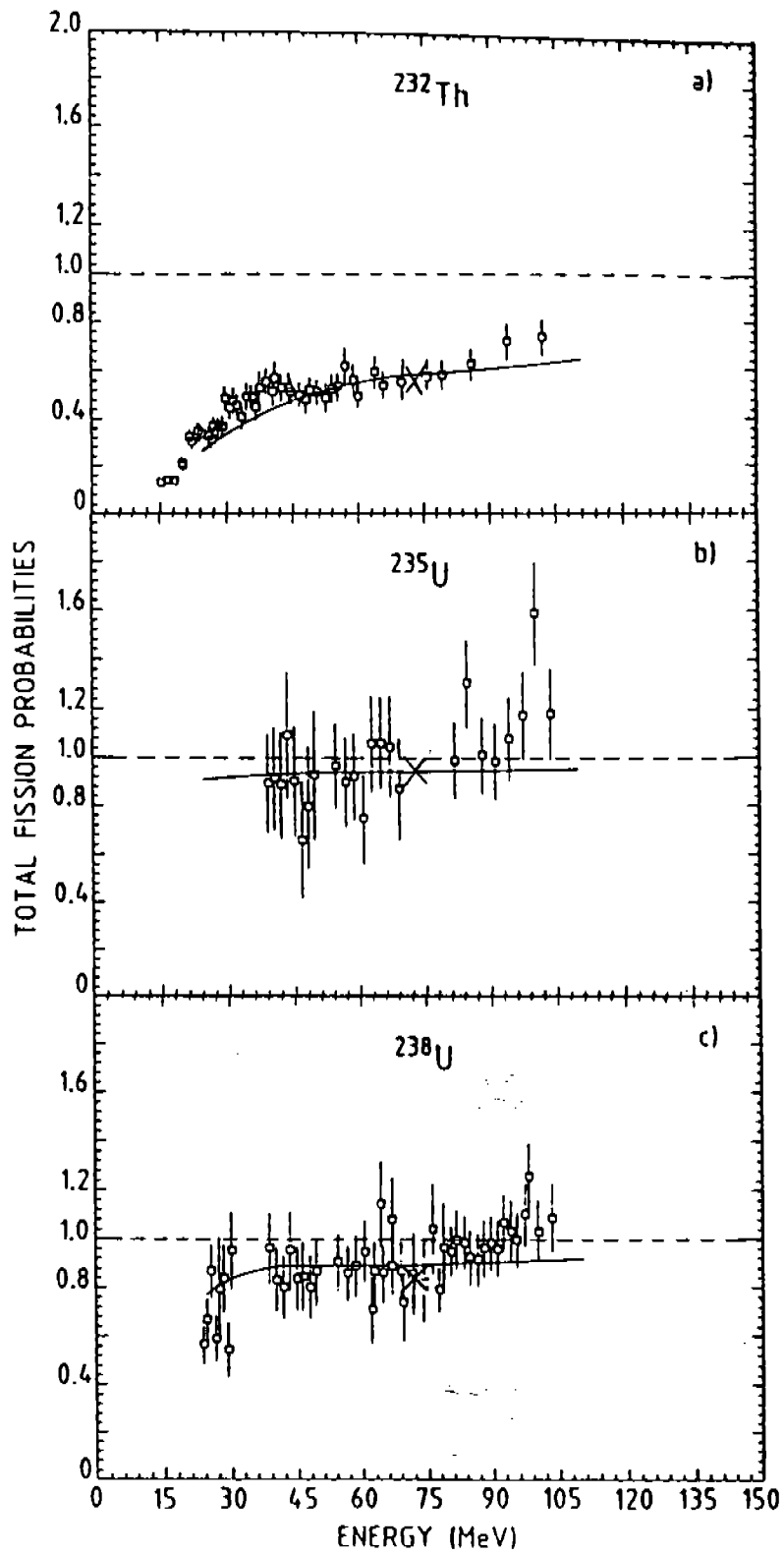


Fig. 15. Experimental total fission probabilities (using the GDR parameters of ref. <sup>5</sup>) and theoretical total fission probabilities; x: simple model; —: hybrid model [ref. <sup>19</sup>] for (a)  $^{232}\text{Th}$ , (b)  $^{235}\text{U}$ , (c)  $^{238}\text{U}$ .

Fig. 6

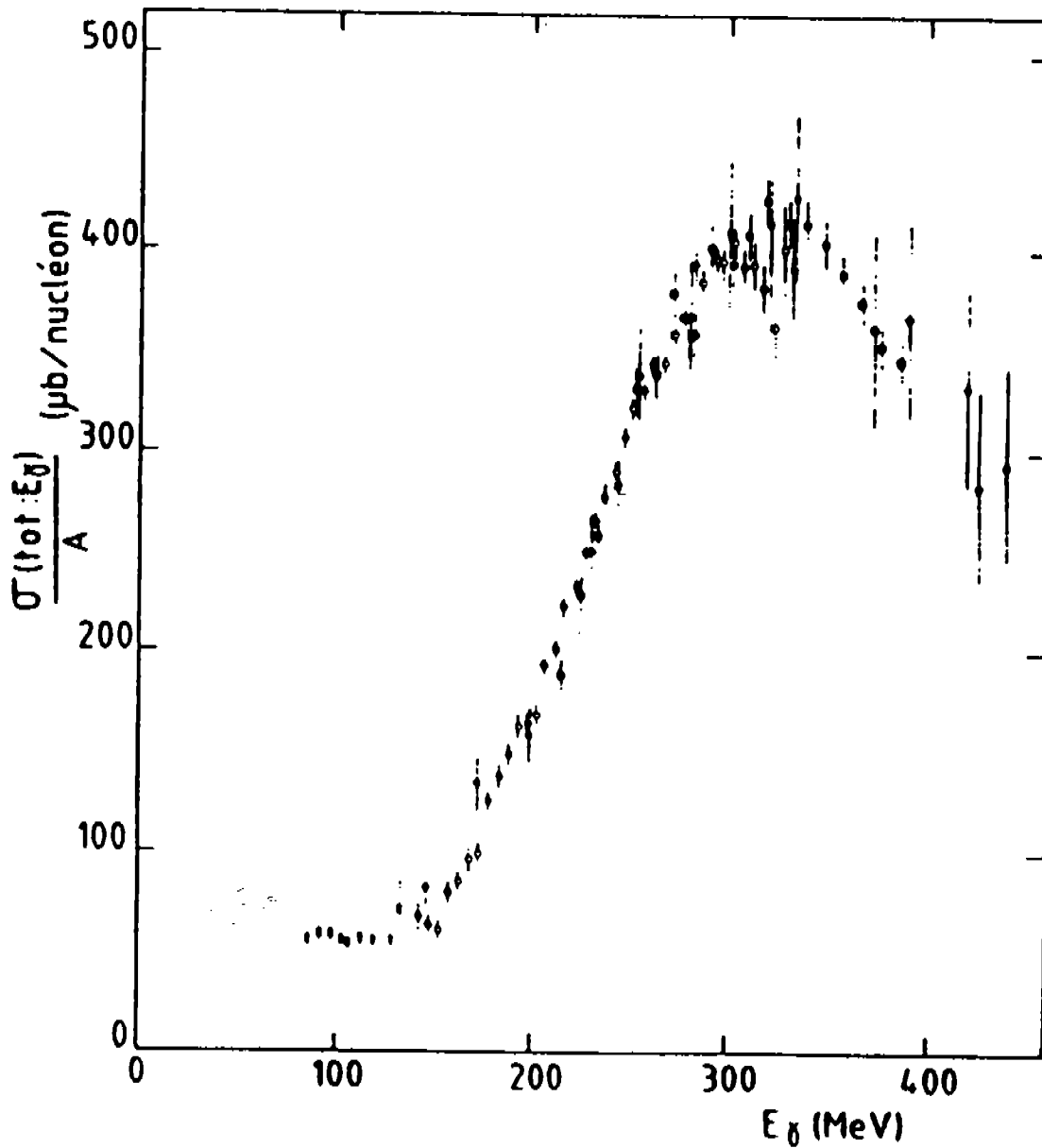


Fig. 4. Comparison of the total photonuclear absorption cross section per nucleon  $\sigma(\text{tot}; E_\gamma)/A$  ( $\mu\text{b}/\text{nucleon}$ ) obtained from: beryllium data  $\phi$  (ref. [5])  $\blacklozenge$  (ref. [6]) (statistical errors only) lead data  $\dagger$  (ref. [9])  $\blacklozenge$  this experiment.

Fig. 7

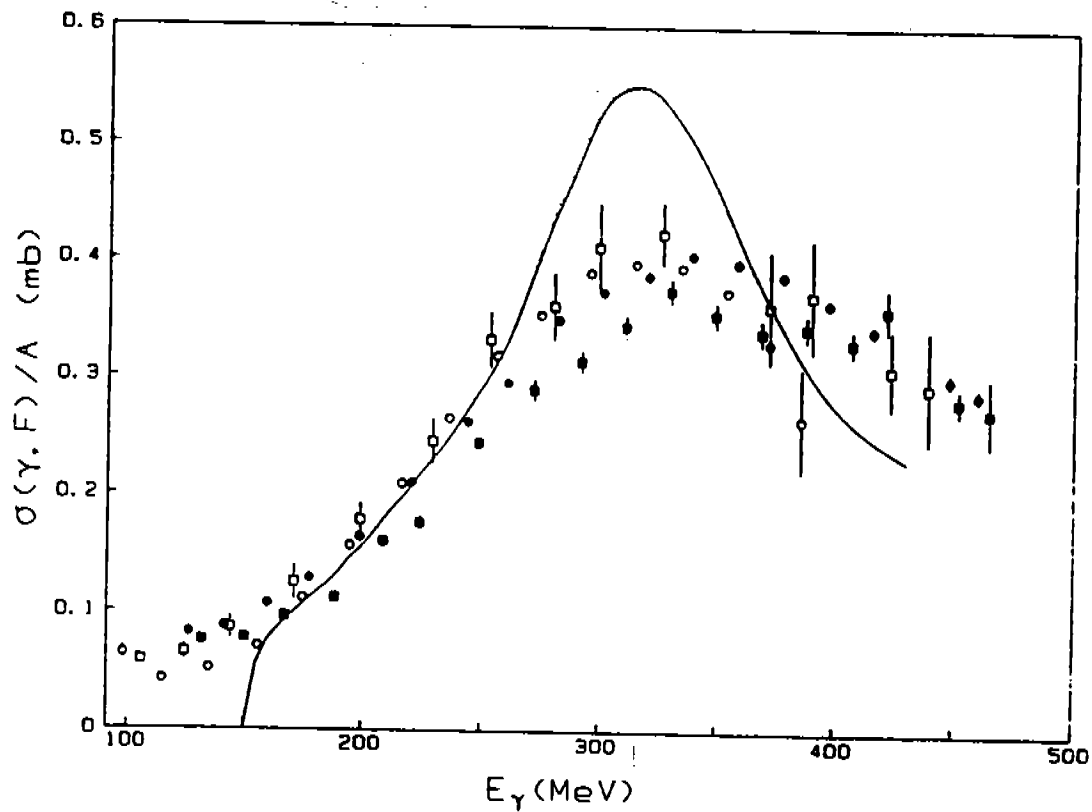


Fig. 4. Comparison of our results for  $^{235}\text{U}(\gamma, F)$  ( $\blacksquare$ ) and  $^{238}\text{U}(\gamma, F)$  ( $\bullet$ ) with total absorption cross sections for the free nucleon (—) from ref. [13],  $^9\text{Be}$  ( $\circ$ ) averaged from ref. [1] and from ref. [2] and  $^{208}\text{Pb}$  ( $\square$ ) from ref. [3]. All data are normalized to the number of nucleons.

Fig. 8

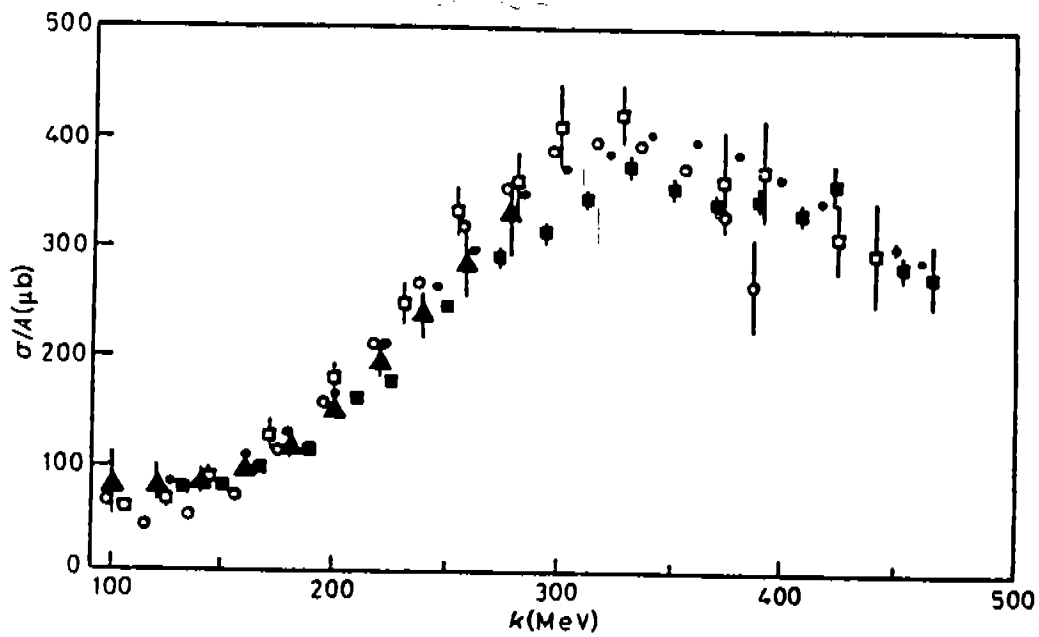
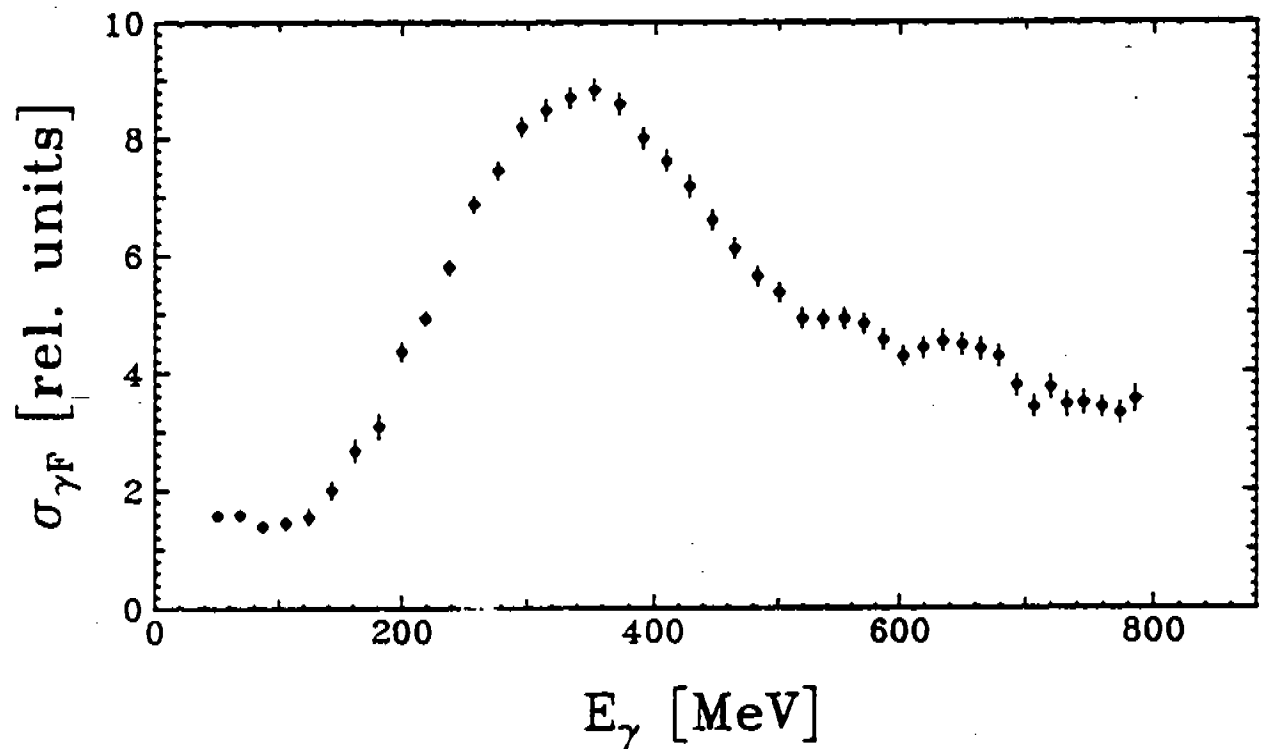


Fig. 7. - Normalized cross-section per nucleon *vs.* the photon energy  $k$ . Our results ( $\Delta$ ) are compared with  $^{235}\text{U}$  ( $\blacksquare$ ) and  $^{238}\text{U}$  ( $\bullet$ ) photofission measurements from ref. (19), and with total photoabsorption cross-sections for  $^9\text{Be}$  ( $\circ$ ), from ref. (33), and  $^{208}\text{Pb}$  ( $\square$ ), from ref. (34) (adapted from ref. (19)).

Fig. 9





First preliminary  $\sigma_{\gamma F}$ -data for  $^{238}\text{U}$  from tagged photon experiments at MAMI B.

Fig. 10

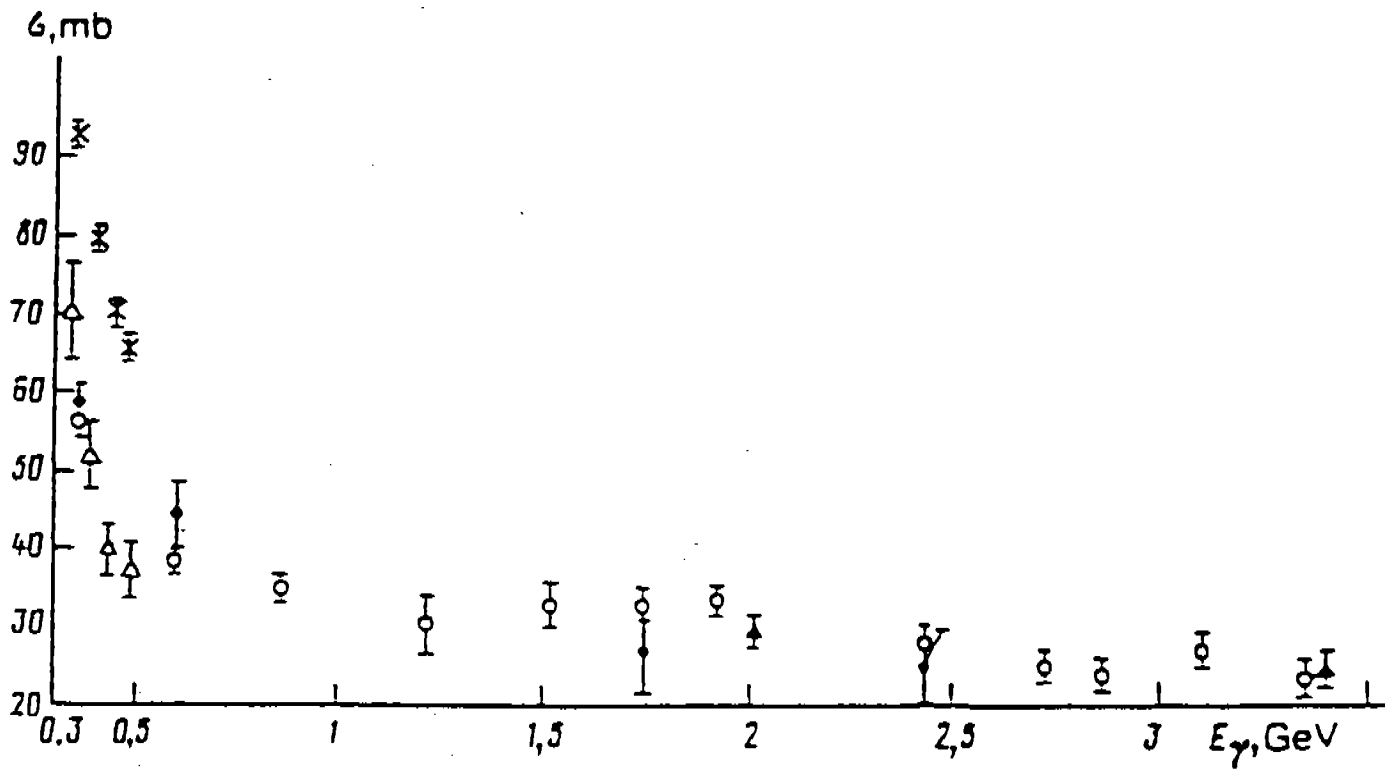


FIG. 2. Energy dependence of the total cross section for hadron production:  $\circ$ - $^{235}\text{U}$ ,  $\bullet$ - $^{238}\text{U}$ ,  $\times$ -Ref. 2,  $\Delta$ -Ref. 18,  $\blacktriangle$ -Ref. 19.

Fig. 11

CU PLATED G-10 BASE PLATE

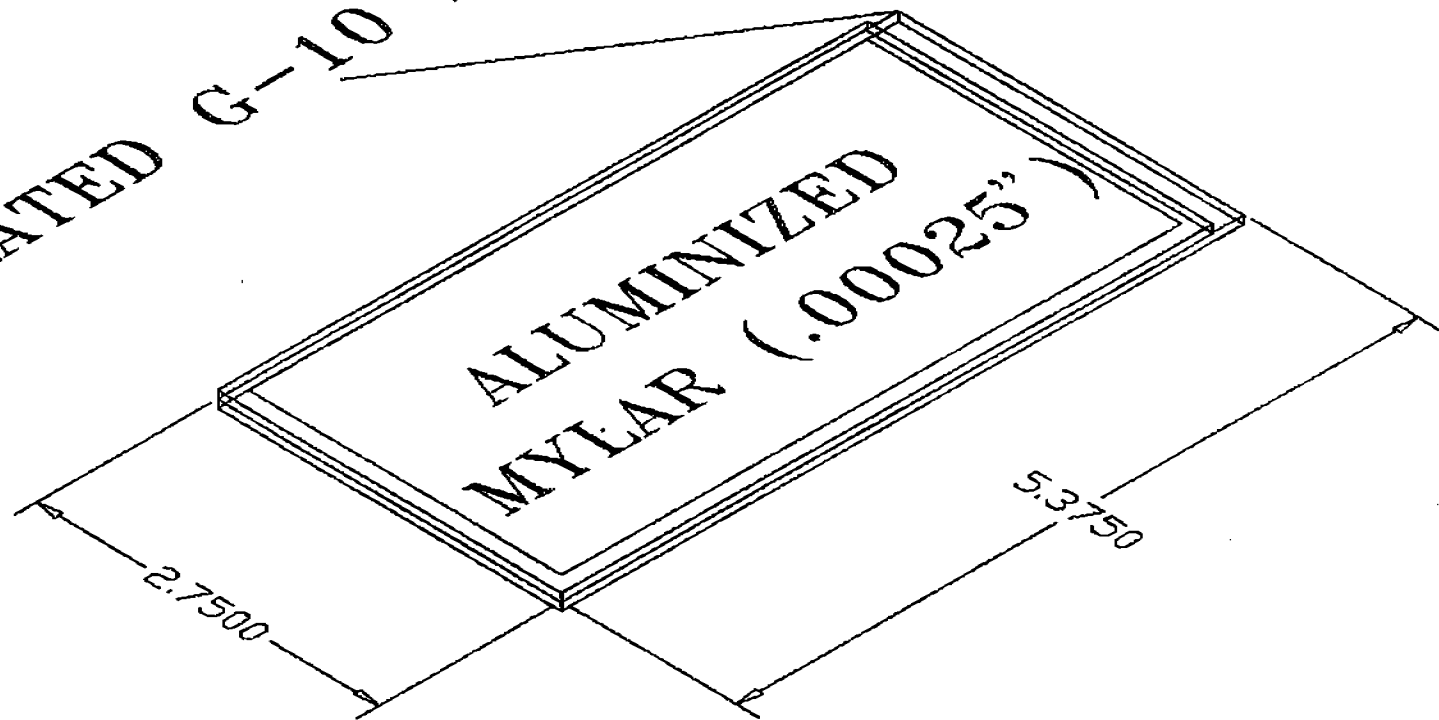


Figure 12. PPACs used in NBL experiment